The Journal of Experimental Biology 216, 4626-4638

doi:10.1242/jeb.093823

RESEARCH ARTICLE

Salinity-induced regulation of the *myo*-inositol biosynthesis pathway in tilapia gill epithelium

Romina Sacchi, Johnathon Li, Fernando Villarreal, Alison M. Gardell and Dietmar Kültz*

Physiological Genomics Group, Department of Animal Sciences, University of California, Davis, One Shields Avenue, Meyer Hall, Davis, CA 95616, USA

*Author for correspondence (dkueltz@ucdavis.edu)

SUMMARY

The *myo*-inositol biosynthesis (MIB) pathway converts glucose-6-phosphate to the compatible osmolyte *myo*-inositol that protects cells from osmotic stress. Using proteomics, the enzymes that constitute the MIB pathway, *myo*-inositol phosphate synthase (MIPS) and inositol monophosphatase 1 (IMPA1), are identified in tilapia (*Oreochromis mossambicus*) gill epithelium. Targeted, quantitative, label-free proteomics reveals that they are both upregulated during salinity stress. Upregulation is stronger when fish are exposed to severe (34 ppt acute and 90 ppt gradual) relative to moderate (70 ppt gradual) salinity stress. IMPA1 always responds more strongly than MIPS, suggesting that MIPS is more stable during salinity stress. MIPS is N-terminally acetylated and the corresponding peptide increases proportionally to MIPS protein, while non-acetylated N-terminal peptide is not detectable, indicating that MIPS acetylation is constitutive and may serve to stabilize the protein. Hyperosmotic induction of MIPS and IMPA1 is confirmed using western blot and real-time qPCR and is much higher at the mRNA than at the protein level. Two distinct MIPS mRNA variants are expressed in the gill, but one is more strongly regulated by salinity than the other. A single MIPS gene is encoded in the tilapia genome whereas the zebrafish genome lacks MIPS entirely. The genome of euryhaline tilapia contains four IMPA genes, two of which are expressed, but only one is salinity regulated in gill epithelium. The genome of stenohaline zebrafish contains a single IMPA gene. We conclude that the MIB pathway represents a major salinity stress coping mechanism that is regulated at multiple levels in euryhaline fish but absent in stenohaline zebrafish.

Supplementary material available online at http://jeb.biologists.org/lookup/suppl/doi:10.1242/jeb.093823/-/DC1

Key words: osmoregulation, compatible osmolytes, fish gill, targeted LC-MS/MS, N-terminal acetylation.

Received 11 July 2013; Accepted 2 September 2013

INTRODUCTION

Our laboratory has previously discovered that *myo*-inositol phosphate synthase (MIPS; EC 5.5.1.4), which is the first enzyme in the *myo*-inositol biosynthesis (MIB) pathway, is transiently induced at the mRNA level in gills of tilapia exposed to acute salinity stress (Fiol et al., 2006). In addition, Kalujnaia and others (Kalujnaia and Cramb, 2009; Kalujnaia et al., 2010) have shown that the second enzyme of the MIB pathway (IMPA; EC 3.1.3.25) is also strongly induced at the mRNA level in the gill, kidney and intestine of European eels. These data on salinity effects at the transcript level suggest that the MIB pathway is physiologically important during osmotic stress because it generates high concentrations of the compatible organic osmolyte *myo*-inositol, which protects cells from salinity-induced damage (Yancey et al., 1982). In addition, *myo*-inositol produced *via* the MIB pathway represents a substrate for the synthesis of phosphoinositide compounds that are implicated in evolutionarily highly conserved signaling pathways, including osmotic stress signaling (Munnik and Vermeer, 2010).

Tilapia represent excellent models for mechanistic studies of osmotic stress signaling pathways. These extremely euryhaline cichlids have evolved in Africa and are now distributed in subtropical and tropical limnic and marine habitats throughout the world. Tilapia tolerate salinities ranging from freshwater (FW) to 120 ppt (Stickney, 1986). Their high salinity tolerance may have evolved as a result of strong selection pressure associated with frequent seasonal droughts and intermittent flooding events in areas characterized by salt-rich bedrock and soil (Costa-Pierce, 2003). Besides inhabiting FW and marine (34 ppt) habitats, tilapia occur in hypersaline desert lakes. For instance, they are found in large numbers in the Salton Sea (Southern California, USA) and its tributaries (Sardella et al., 2004; Sardella and Brauner, 2007). The Salton Sea is hypersaline, having an average salinity of 50 ppt with salinity in some areas increasing to 100 ppt during seasonal droughts (Miles et al., 2009). Therefore, studies investigating how tilapia respond to such hypersaline conditions are not only informative for dissecting the mechanisms of euryhalinity and extreme osmotic stress tolerance, but they are also relevant from an ecophysiological perspective. The present study utilizes a targeted proteomics approach consisting of online liquid chromatography–tandem mass spectrometry (LC-MS/MS) and utilization of accurate mass and time tags (AMT) (Cutillas and Vanhaesebroeck, 2007; Andreev et al., 2012; Matzke et al., 2013) to quantify both enzymes of the MIB pathway in gills of Mozambique tilapia [*Oreochromis mossambicus* (Peters 1852)] after exposure to different types of salinity stress. Changes in protein abundance in response to environmental stress can occur as a result of increasing the corresponding mRNA to increase translation (Gracey et al., 2001), but may also be a result of protein (de)stabilization and altered rates of turnover (Flick and Kaiser, 2012). To assess the contribution of transcriptional regulation in the stress-related alteration of protein levels, it is critical to quantify the

abundance of the corresponding transcripts. Interestingly, correlative regulation of mRNA and protein abundances in response to environmental stress is often fractional, i.e. mRNA responses are either more or less pronounced than protein responses. Sometimes, correlation between the regulation at mRNA and protein levels is lacking altogether. Changes in mRNA but not protein abundance may compensate for changes in translational efficiency or protein degradation rates to keep protein levels constant (Schwanhäusser et al., 2013). Alternatively, protein abundance changes can occur without altering the corresponding mRNA level by regulation of protein degradation or microRNA effects on translational efficiency (Selbach et al., 2008).

Effects of salinity stress on mRNA and protein abundances have been documented for many genes, and this mechanism of regulation represents a major pillar of salinity stress responses in fish and other organisms (Fiol et al., 2006; Evans and Somero, 2008; Dowd et al., 2010). However, alternative mechanisms such as post-translational modification (PTM) and alternative splicing also play crucial roles in salinity stress responses. For instance, protein phosphorylation is a common PTM that affects many fish proteins during salinity stress (Kültz and Burg, 1998; Kültz and Avila, 2001; Marshall et al., 2009). In addition, alternative splicing of tilapia prolactin receptor 2 and the murine homolog of osmotic stress transcription factor 1 (OSTF1/TSC22D3) have been observed in response to salinity stress (Fiol et al., 2007; Fiol et al., 2009). The present study investigates the mechanisms by which euryhaline tilapia regulate the MIB pathway during different types of salinity stress, including the regulation of protein and mRNA abundances, PTM (specifically N-terminal protein acetylation), and alternative transcript splicing and isoform expression of MIB pathway enzymes. The relationship between MIB pathway regulation at the mRNA and protein levels and the evolutionary implications of MIB pathway regulation for osmoregulation and salinity adaptation of euryhaline fish are discussed.

MATERIALS AND METHODS

Tilapia salinity acclimation

Adult Mozambique tilapia (*O. mossambicus*) were grown and maintained at the UC Davis Center for Aquatic Biology and Aquaculture in 114 l recirculating aquaria at 26°C. Several salinity acclimation experiments were conducted in which fish (both sexes equally distributed among experimental groups) were exposed to either a two-step acute salinity increase from 0.4 ppt [=freshwater (FW)] to 34 ppt (17 ppt day^{-1}), a gradual salinity increase from FW to 70 ppt (7 ppt day^{-1}) or a gradual salinity increase from FW to 90 ppt (7 ppt day^{-1}). The age of the fish was between 6 and 8 months at the start of the experiments and the duration of the experiments was between 2 days (34 ppt) and 2 weeks (90 ppt). Salinity was increased using Instant Ocean sea salt (Spectrum Brands, Blacksburg, VA, USA) and monitored using a conductivity meter (YSI, Yellow Springs, OH, USA). All three acclimations were accompanied by handling controls using FW instead of saline for daily water changes. Fish were sampled by over-anesthesia with MS-222 and spinal transection. Gill epithelium was immediately collected, divided into aliquots, snap-frozen in liquid nitrogen, and stored at −80°C. All animal procedures were approved by the UC Davis Institutional Animal Care and Use Committee (IACUC protocols 13468 and 15013, assurance number A3433-01).

Protein extraction and in solution digestion

Tissue homogenization, protein extraction and in-solution digestion procedures were extensively optimized to yield quantitatively reproducible LC-MS/MS data and minimize protein modification during processing (Kültz et al., 2013). Each sample was homogenized under liquid nitrogen in a mortar and pestle. The tissue powder was transferred immediately to a low-retention microcentrifuge tube (Eppendorf, Hauppauge, NY, USA), and proteins were extracted and precipitated with 10% trichloroacetic acid, 90% acetone and 0.2% dithiothreitol (DTT), washed twice with 100% acetone and 0.2% DTT, and solubilized in 7 mol l^{-1} urea, 2 mol l^{-1} thiourea and 0.2% DTT. Insoluble material was removed by centrifugation at 18,000 ***g*** for 5 min and transfer of the clear supernatant into a new low-retention microcentrifuge tube. Ten microliters were removed for protein assay and the remainder was frozen at −80°C. Protein assay was performed using a 10× aqueous dilution of sample at A660 nm with an assay that is compatible with urea, thiourea and DTT (cat. no. 22660, Thermo Fisher Scientific, Rockford, IL, USA). For in solution digestion 100 µg total protein was diluted 1:1 in LC-MS water (Optima W6-1, Thermo Fisher Scientific) and mixed with 1/10th volume 1 mol l^{-1} triethanolamine (pH 8.0) in a 0.6 ml low-retention microcentrifuge tube. Protein was reduced by adding 5% (v/v) of 80 mmol l^{-1} DTT and incubating at 55°C for 30 min. Reduced protein was alkylated by adding 16.8% (v/v) of 100 mmol l^{-1} iodoacetamide (IAA) and incubating in the dark for 30 min. Immobilized trypsin (cat. no. V9012, Promega, Madison, WI, USA) was added at a ratio of 1:25 (4 µg) and allowed to digest proteins for exactly 16 h at 35°C. Trypsin was removed by centrifugation at 18,000 ***g*** for 2 min. After drying the sample by SpeedVac peptides were resuspended in 200 µl of 0.1% formic acid in LC-MS water and the solution was transferred to a maximum recovery vial (cat. no. 186005670CV, Waters, Milford, MA, USA), which was stored at −80°C.

Label-free quantitative proteome profile analysis

Gill samples from 36 animals were analyzed (six biological replicates each for 34, 70 and 90 ppt acclimation groups and another 18 for corresponding FW handling controls). Trypsin-digested peptides were separated by nanoAcquity UPLC (LC, Waters) using a Symmetry C18 Trap column (cat. no. 186003514, Waters) and a BEH C18 separating column (cat. no. 186003545, Waters). A 70 min linear gradient of 3–35% acetonitrile (20 min injection delay) was used for LC. A micrOTOF-QII mass spectrometer (Bruker Daltonics, Bremen, Germany) was connected online to the LC *via* a dual picoemitter tip (New Objective, Woburn, MA, USA) nano-electrospray ionization source (Bruker Daltonics). One spray line was used for sample elution, the other (*via* a secondary auxillary pump line of the LC) for delivering ESI-L Low Concentration Calibrant Mix (cat. no. G1969-85000, Agilent Technologies, Santa Clara, CA, USA) during each sample's injection delay. This arrangement allowed for accurate internal mass calibration of every sample, which outperformed using a single lock mass. micrOTOF-Control 3.0 and Hystar 3.2 (Bruker Daltonics) were used to automate acquisition of spectra. Each sample was analyzed by DataAnalysis 4.0 (Bruker Daltonics), which included deconvolution, MS/MS compound finding and MS molecular feature recognition.

A database consisting of the complete Nile tilapia (*Oreochromis niloticus*) proteome plus all available sequences for *O. mossambicus* (28,020 total sequences downloaded from UniProtKB on 29 July 2012) was complemented with a decoy database containing a randomly shuffled entry of each sequence (generated by Phenyx 2.6.2, GeneBio, Geneva, Switzerland). MS/MS compounds were then searched in Proteinscape 3.1 (Bruker Daltonics) against this combined decoy database (56,040 total sequences) using the Mascot 2.2.7 (MatrixScience, Boston, MA, USA) (Koenig et al., 2008)

and Phenyx 2.6.2 (Masselot et al., 2004) search engines (false discovery rate <2%). The following parameters were used: enzyme specificity=trypsin, missed cleavages permitted=1, fixed modification=Cys carbamidomethylation, variable modifications=Met oxidation and Pro hydroxylation, precursor ion mass tolerance=20 ppm, fragment ion mass tolerance=0.1 Da. A threshold score of 5% probability that a protein identification is incorrect was used for accepting individual MS/MS spectra. Search results were assessed and combined in Proteinscape 3.1 (Bruker Daltonics, Bremen, Germany). To comply with MIAPE (Minimum Information About a Proteomics Experiment) guidelines (Taylor et al., 2007; Binz et al., 2008; Taylor et al., 2008), search parameters, line spectra, quality control criteria and identifications were deposited in the PRIDE repository and can be accessed using PRIDE Inspector (accession numbers 28622–28631) (Côté et al., 2012; Csordas et al., 2012; Wang et al., 2012; Csordas et al., 2013; Vizcaíno et al., 2013). MS molecular features identified with DataAnalysis 4.0 were imported into ProfileAnalysis 2.0 (both Bruker Daltonics) and comparison of peptide abundances in treated *versus* control samples was performed by quantitation of chromatographic peak area integrals of peptides with matching retention time (Rt) and mass over charge ratio (*m*/*z*). Abundance ratios for each peptide meeting those criteria were imported and matched to MS/MS protein IDs in Proteinscape 3.1 (Bruker Daltonics). Matching criteria consisted of an Rt deviation maximum of 1 min and an *m*/*z* deviation maximum of 0.02 Da.

Targeted LC-MS/MS quantitation of IMPA1 and MIPS protein regulation

All IMPA1 (UniProtKB accession number Q3ZLD0) and MIPS (UniProtKB accession number Q1KN76) peptides identified by LC-MS/MS were evaluated for their potential as diagnostic indicator ions for targeted quantitation. The criteria for peptide evaluation included absence of PTMs (except for Cys carbamidomethylation), high MS/MS ion scores, high Rt reproducibility, no missed or unspecific cleavage, no alternative sequence assignment, and no ambiguity regarding protein ID assignment. The threshold mass accuracy and Rt reproducibility for this analysis were set to 0.02 Da and 0.7 min, respectively. Because gill samples were highly complex, all extracted ion chromatograms (EICs) were visually inspected for overlap with neighboring peaks. If an overlapping adjacent peak was observed within Rt ± 0.7 min for any sample or if there were multiple missing values per group, then the corresponding peptides were excluded from targeted quantitation. Visual inspection also served to verify that for each peptide all 12 EIC peaks (six treated and six controls) fall within the range of mean Rt ± 0.7 min as calculated by Proteinscape 3.1. Peptide EICs were automatically integrated using DataAnalysis 4.0 and the quantity of peptides was calculated as the ratio of the corresponding EIC integral relative to the mean of the six FW controls. This procedure was repeated for the base peak chromatogram integral of each sample, which served for normalization of peptide quantities across all samples within an experiment. A two-factor ANOVA with replication was performed after normalization to discern whether treatment effects were significant, considering all peptide abundances per protein.

Western blot analysis

Total protein was extracted from gill epithelium by grinding the frozen tissue with a glass pestle in a glass homogenizer on ice. RIPA buffer containing phosphatase and protease inhibitors {50 mmol l^{-1} Tris-HCl pH 7.5, 150 mmol l^{-1} NaCl, 1% NP-40, 1% Triton X-100, 2% 3-[(3-cholamidopropyl)dimethylammonio]-1-propanesulfonate (CHAPS), 4 mmol l^{-1} NaF and 2 mmol l^{-1} activated Na_3VO_4, complete Ultra tablet protease inhibitor cocktail (Roche, Basel, Switzerland)} was used for tissue homogenization. Tissue homogenates were centrifuged at 19,000 ***g*** and 4°C, and the supernatant was transferred to a low protein binding tube. Total protein was quantified by bicinchoninic acid protein assay. A homogenate aliquot containing 35 µg total protein was then mixed with Laemmli buffer (1:2 ratio) containing 100 mmol l^{-1} DTT and heated at 90°C for 3 min before loading on a 15% SDS-PAGE gel. Recombinant, hexa-His-tagged *O. mossambicus* MIPS and IMPA1 proteins were expressed in *Escherichia coli*, affinity-purified using nickel columns (F.V., unpublished), and loaded as controls to confirm the expected molecular weight. Pre-stained molecular weight markers (10–250 kDa, Kaleidoskope, Bio-Rad, Hercules, CA, USA) were also loaded in the first lane on each gel. Electrophoresis was performed in running buffer (25 mmol l^{-1} Tris, 192 mmol l^{-1} glycine, 0.1% SDS) at 120 V constant voltage until the SDS front reached the bottom of the gel. Once electrophoresis was complete, one gel was subjected to Coomassie Blue staining and the other was transferred to PVDF membrane using a semi-dry transfer system (Trans-Blot SD Cell, Bio-Rad). Membranes were blocked with 3% nonfat dry milk (NFM) in TBS (50 mmol l^{-1} Tris-HCl pH 7.4, 150 mmol l^{-1} NaCl) buffer containing 0.05% Tween-20 (TBST) for 1 h at room temperature. Membranes were then incubated with rabbit anti-human MIPS (sc-134687, Santa Cruz Biotechnology, Dallas, TX, USA), goat anti-human IMPA1 (sc-50596, Santa Cruz Biotechnology, Dallas, TX, USA) or goat anti-human actin (sc-1615, Santa Cruz Biotechnology) at 1:250, 1:250 or 1:400 dilution, respectively, in 3% NFM-TBST for 1.5 h at room temperature. After washing the membranes three times with TBST for 10 min they were incubated for 1 h at room temperature with the peroxidase-conjugated secondary antibodies, donkey anti-goat or goat anti-rabbit, at a dilution of 1:5000 in 3% NFM-TBST. Membranes were washed again as described above and antibody-reactive bands were visualized by chemiluminescence detection using Super Signal West Femto Substrate (Thermo Fisher Scientific, Rockford, IL, USA).

Identification and quantitation of MIPS N-terminal acetylation

Peak lists were generated using Mascot Distiller 2.4.3 (Matrixscience, Boston, MA, USA) and imported into Phenyx 2.6.2

Table 1. Primers used in semi-quantitative and quantitative real-time PCR on *Oreochromis mossambicus* target cDNA

Target cDNA	Forward (5′ to 3′)	Reverse (5′ to 3′ antisense)	Product (bp)
MIPS-160	CAGAGTCGCGCAGACAATGT	CGTTGACCCCTGGGATGATA	164 and 251
MIPS-250	GTGCATGATCTTCCAGATGGAGCG	AGAAGCGCTCGGTGTTGGCG	110
IMPA1	CGAAACTCTCCTAAGCAAGCCCCC	CCAGCTTTCCTAATTTCCGCGCCA	114
IMPA2	TACCAGAATCCTCTTCTTGGCCACACC	ACCAGGACACTGATGCACAGCTA	121
beta-Actin	CCACAGCCGAGAGGGAAAT	CCCATCTCCTGCTCGAAGT	104
18S rRNA	CGATGCTCTTAGCTGAGTGT	ACGACGGTATCTGATCGTCT	260

(Masselot et al., 2004), PeaksSuite 6 (BSI, Waterloo, ON, Canada) (Zhang et al., 2012), Mascot 2.2.7 (Koenig et al., 2008) and X!Tandem CYCLONE 2010.12.01.1 (www.thegpm.org/tandem) (Craig and Beavis, 2004). They were analyzed against the tilapia database consisting of 50% decoy entries using the same parameters as described above, except that protein N-terminal acetylation was included as an additional variable modification. Results from all four search engines were consolidated in Scaffold 4.0.5 (Proteome Software, Portland, OR, USA) (Searle and Turner, 2006) and metascores obtained by each search engine were recorded for IMPA1 and MIPS peptides, including the N-terminally acetylated MIPS peptide. The consolidated search results were exported as mzid format and then imported into ScaffoldPTM 2.1.1 (Proteome Software), which was used to determine the confidence score for assigning a specific modification to a particular amino acid (A-score) and localization probability for acetylation of the MIPS N-terminal peptide (Beausoleil et al., 2006). In addition, MS/MS spectra of MIPS N-terminal peptides were manually inspected to confirm N-terminal acetylation.

RNA purification and cDNA synthesis

Total RNA was purified from gill epithelium using RNeasy Plus (Qiagen, Hilden, Germany). Briefly, 20–30 mg frozen tissue was disrupted with a RNase-free mortar and pestle, lysed with 600 µl lysis buffer (containing guanidine-isothiocyanate) and homogenized with a QIAshredder (Qiagen). Genomic DNA (gDNA) was removed by passing the lysate through a gDNA eliminator spin column and total RNA was purified by selective binding to a silica-gel membrane spin column (Qiagen). RNA concentration and purity was checked using a NanoDrop spectrophotometer (Thermo Fisher Scientific) at A260, A280 and A320 nm. All A260/A280 ratios obtained were between 2.0 and 2.2. High quality of extracted RNA was also verified on 2% agarose gels. To ensure complete DNA removal, purified RNA was subjected to DNase treatment with TURBO-DNAfree reagent (Life Technologies, Grand Island, NY, USA). gDNA extracted from tilapia blood was used for DNase control reactions to validate proper activity of the DNase enzyme. Two micrograms of DNase-treated total RNA were reverse transcribed in the presence of oligo(dT) and random hexamers in a 1:1 ratio using SuperScript III First-Strand Synthesis kit (Life Technologies). PCR amplifications of target cDNA were performed by combining 2 µl of undiluted cDNA and 10 pmol of each of the corresponding primers (Table 1) in a final volume of 25 µl reaction of PCR Master Mix (Promega, Madison, WI, USA). Cycling conditions were as follows: initial denaturation at 94°C for 1 min followed by 30 cycles of denaturation at 94°C for 30 s, annealing at 60°C for 30 s and extension at 72°C for 1 min. The last cycle was followed by a final extension at 72°C for 5 min. The same primers and conditions were used to amplify gDNA. Five microliters of each PCR product were analyzed by agarose gel (2%) containing GelRed to visualize amplicons for evaluation of purity and size.

Cloning and sequence analysis of MIPS and IMPA

To clone *O. mossambicus*, MIPS and IMPA1 PCR products were amplified from both cDNA and gDNA and fractionated on a 2% agarose gel. Resulting bands were excised from the gel, placed in separate microcentrifuge tubes and incubated at 65°C until the gel slice melted. Then, 4 µl of the melted agarose containing each PCR product was cloned into 2.1-TOPO vector using a TOPO TA cloning strategy. The cloning reaction was followed by chemical transformation of One Shot Mach-T1 Competent cells according to the manufacturer's instructions (Life Technologies). Clones were

Table 2. Identification data for MIPS and IMPA1 peptides that are valid for targeted quantitation and for N-terminally acetylated peptide of MIPS

Protein/ Accession number	Sequence	Start	End	*m/z*	Rt (min)	Mass (Da)	Error (ppm)	z	Protein scape	Ion score				Profile Analysis ratio		
										PEAKS	Phenyx z	Mascot	XITandem	34 ppt/ FW	70 ppt/ FW	90 ppt/ FW
MIPS/Q1KN76	M.S(+42.01)VNVHINSPNVK.Y	2	13	675.3632	33.9	1348.71	0.6	2+		225.19	12.86	68.31	2.8E-08			
	R.TTEMTIR.T	43	49	426.2187	63.2	850.42	1.1	2+	106.4		13.3	53.0		1.2		
	R.DLLPMVHPNDIVFDGWDISSLDLGSAMER.A	125	153	1081.5181	58.3	3241.54	−2.9	3+	80.4	18.61	8.3	43.12	9.7E-06	↑		
	R.ADNVLTGTMAEQMER.I	192	206	833.3818	39.1	1664.75	−0.4	2+	113.4	62.65	11.6	58.82	2.2E-06			
	K.VIVLWTANTER.F	223	233	651.3653	41.4	1300.71	1.6	2+	87.8	37.61	6.6	61.62	5.0E-02			
	R.GVFIGGDDFK.S	259	268	527.7670	37.8	1053.51	5.9	2+	64.9	40.05	5.8	41.80	6.2E-03			
	R.ASIENIMR.A	447	454	467.2478	35.1	932.47	6.6	2+	52.4	34.97	4.0	36.64				
IMPA1/Q3ZLD0	R.YDFAVAVAR.K	8	17	541.7850	39.0	1081.56	−0.2	2+	92.4	53.72	8.4	49.58	5.4E-02	0.9	1. 5	6.4
	K.IIIGSLK.E	53	59	372.2546	36.4	742.5	−0.8	2+	55.4	16.15	3.4	48.35				
	K.SIISEHGTDR.S	159	169	614.3193	30.7	1226.64	−1.1	2+	54.9	17.97	6.2	26.25	3.5E-02			↑
	K.IFSTMQK.M	177	183	427.7252	30.8	853.44	−1.1	2+	20.9	19.72	5.2					↑
	R.MVSANNETIAK.R	252	262	589.2972	29.0	1176.58	−0.7	2+	88.4	59.51	8.4	55.28	8.3E-03	1.3		↑
	K.EIEIFPVVR.D	267	275	551.3210	45.9	1100.62	4.1	2+	77.3	42.9	6.5	51.38		1.1		↑

Peptide information, including retention time (Rt) and peptide ion scores obtained with multiple search engines, is shown. In addition, semi-quantitative ProfileAnalysis ratios of estimated MIPS and IMPA1 abundances in gills from salinity-stressed *versus* freshwater (FW) control tilapia are included when available. An upward arrow indicates an extreme ProfileAnalysis ratio, i.e. the peptide was only quantified in samples from salinity stressed fish because it did not meet the ProfileAnalysis threshold criteria (see Materials and methods) in FW controls.

screened by PCR and sequenced using M13 and M13 reverse primers. Sequences were analyzed by nucleotide alignment using Geneious Pro 5.1.7 (Biomatters, Auckland, New Zealand). For MIPS, the sequence stretch unique to the long transcript was targeted for designing long MIPS variant-specific PCR primers (Table 1). Using these primers resulted in amplification of a single PCR product. Discontiguous megablast searches against the GenBank RefSeq genomes and transcriptomes of *O. niloticus* and *Danio rerio* were performed on 6 July 2013. These BLAST searches served to identify the number of tilapia and zebrafish MIPS and IMPA loci that are homologous to *O. mossambicus* MIPS (GenBank accession number DQ465381) and IMPA1 (GenBank accession number JQ943581). For phylogenetic analysis, MIPS and IMPA protein sequences from fish and other species were obtained by searching NCBI, UniProt and Ensembl databases. Multiple sequence alignment and phylogenetic tree construction using a distance-matrix (neighbor-joining) method with bootstrapping (1000 iterations) were performed using Geneious Pro 5.1.7.

Quantitative real-time PCR

Relative expression levels of MIPS-160 and MIPS-250 transcripts and IMPA1 and IMPA2 mRNAs in salinity treated samples *versus* FW controls were quantified by qPCR on a 7500 Fast Real-Time PCR system (Life Technologies, Grand Island, NY, USA). Each sample was run in triplicate. Reactions were prepared using 2 µl of 1:10 dilution of cDNA samples to amplify target cDNAs (1:1000 dilution for highly abundant 18S rRNA), 5 pmol of each primer, 6 µl of nuclease-free water and Fast SYBR Green Master Mix reagent to a final volume of 20 µl as recommended by Applied Biosystems. Cycling conditions were: one cycle at 95°C for 20 s followed by 40 cycles of 95°C for 3 s and 60°C for 30 s. Melt curve analysis was performed at the end of each PCR reaction. Appropriate controls (no reverse transcriptase, no template, DNase treatment controls) were included in triplicate in each experiment. The same fish were analyzed for changes in mRNA and protein expression. The $\Delta\Delta C_t$ method (Pfaffl, 2001) was used to calculate the ratio of MIPS and IMPA mRNAs in salinity-acclimated fish relative to FW handling controls. The mean of two stably expressed RNAs (beta-actin mRNA and 18S rRNA) was used for data normalization (arithmetic and geometric means yielded the same results). Individual PCR amplification efficiencies were calculated for each sample using LinRegPCR software (Ruijter et al., 2009). They were between 1.90 and 1.95 in each case and were unaltered by salinity treatments. A Mann–Whitney *U*-test (Wilcoxon rank sum test) was

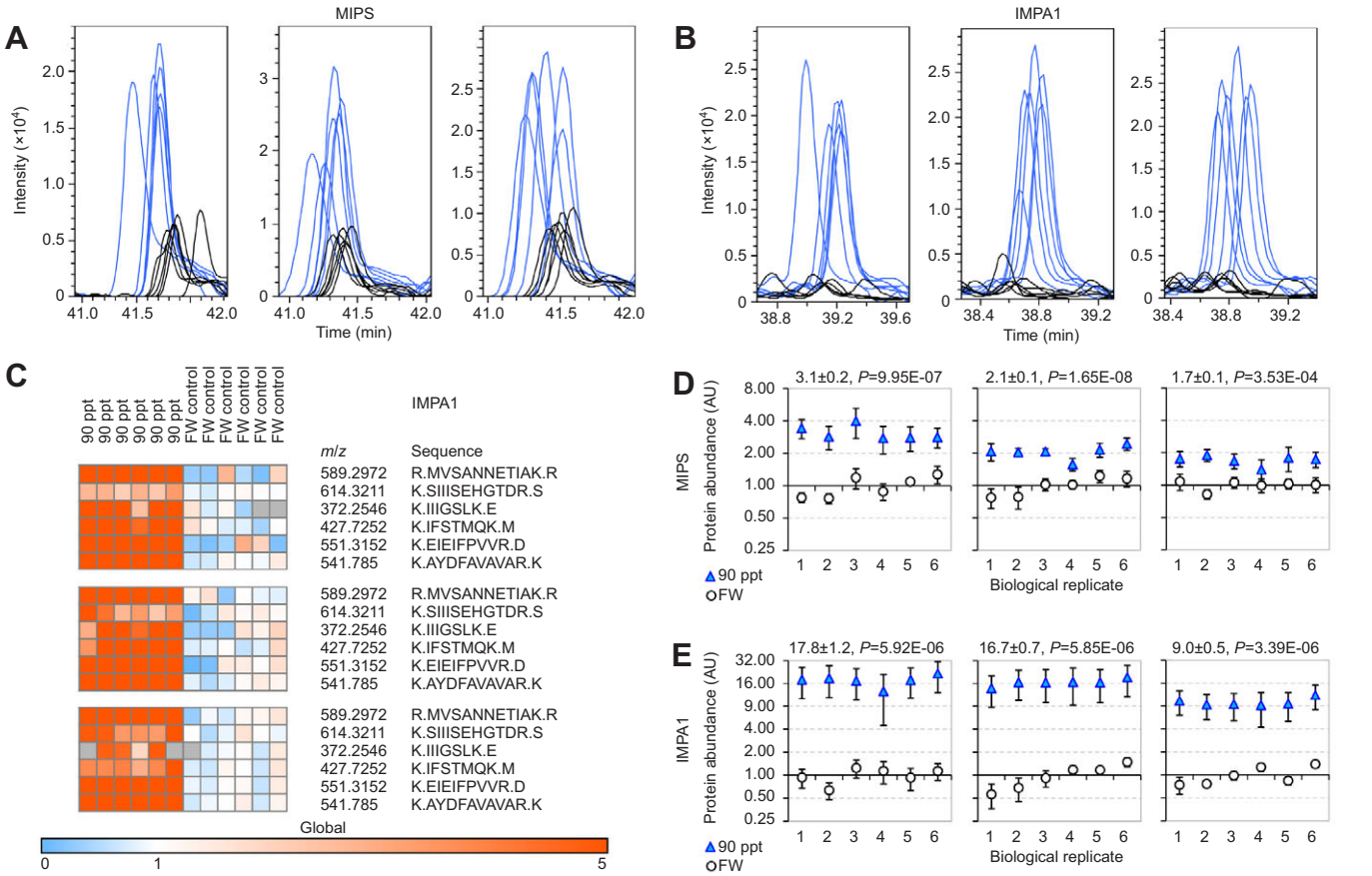

Fig. 1. Targeted quantitation of *myo*-inositol phosphate synthase (MIPS) and inositol monophosphatase 1 (IMPA1) abundances in gill epithelium of tilapia exposed to 90 ppt compared with freshwater (FW) handling controls. (A,B) Extracted ion chromatograms (EICs) for MIPS peptide VIVLWANTER *m/z* 651.3653 (A) and IMPA1 peptide AYDFAVAVAR *m/z* 541.7850 (B). EIC traces for six samples from 90 ppt acclimated fish are shown in blue and EIC traces for six FW control samples are shown in black. Three technical replicates are depicted horizontally. (C) Heat map illustrating the abundance difference between samples from 90 ppt acclimated tilapia and FW handling controls for all IMPA1 diagnostic peptides. Three technical replicates are depicted vertically. The heat map was generated using Gene-E (BROAD Institute, Cambridge, MA, USA). (D,E) Protein abundances of six biological replicates for MIPS (D) and IMPA1 (E). Each data point represents the mean ± s.e.m. abundance of all diagnostic peptides for a single biological replicate, and *y*-axes are plotted on a $\log_2$ scale. Three technical replicates are depicted horizontally. The protein mean ± s.e.m. of all six biological replicates for salinity-stressed fish and the *P*-value for the two-factor ANOVA are shown at the top of each chart.

performed on the normalized data to determine whether mRNA abundances in treated *versus* control samples were statistically different (P<0.05). The mRNA abundances ratio of the two MIPS transcript variants was calculated using Eqn 1:

$$\text{Ratio} = \frac{E_{\text{MIPS-160}} C_{t_{\text{MIPS-160}}}}{E_{\text{MIPS-250}} C_{t_{\text{MIPS-250}}}}, \quad (1)$$

where E is the amplification efficiency and C_t is the cycle number at the threshold fluorescence.

RESULTS

Identification of MIPS and IMPA1 by LC-MS/MS

Three unbiased label-free quantitative gill proteome profile analyses were performed to identify salinity-regulated proteins, and *O. mossambicus* MIPS (UniProt accession number Q1KN76) and IMPA1 (UniProt accession number Q3ZLD0) were revealed as candidates. The cDNA sequences corresponding to those proteins were previously cloned and submitted to GenBank by our laboratory (GenBank accession numbers DQ465381 for MIPS and JQ943581 for IMPA1). All proteins identified in the three proteome profile analyses, pertinent metadata, identification scores, spectra and quality control criteria have been deposited in the public PRIDE repository (PRIDE accession numbers 28622–28631). Quantitatively diagnostic MIPS and IMPA1 peptides, their identification scores and ProfileAnalysis 2.0 ratios (if available) are shown in Table 2. These data illustrate that MIPS and IMPA1 can be readily detected by LC-MS/MS. In addition, their semi-quantitative ProfileAnalysis ratios suggest that both proteins increase in abundance during 90 ppt salinity stress compared with FW controls. However, in particular for MIPS, a quantitative ProfileAnalysis ratio was missing for most peptides because the corresponding peptide quantities were not matched to the protein ID. Moreover, often the dynamic range for determining a ratio with global profile analysis was insufficient to identify MIPS or IMPA1 peptides in FW controls because the intensity threshold for detecting a peak in the global profile analysis had to be set high (>1000 counts) to minimize artifacts. Therefore, targeted label-free proteomics based on LC-MS/MS and the AMT approach was performed on diagnostic peptides identified for MIPS (excluding the N-terminal peptide) and IMPA1 (Table 2).

Upregulation of MIPS and IMPA1 proteins by 90 ppt salinity stress

Targeted AMT was initially performed for samples from tilapia exposed to 90 ppt and the corresponding FW handling controls because global profile analysis data indicated that the effect of salinity was strongest under these conditions (Table 2). The LC-MS/MS retention time reproducibility between biological and technical replicates as illustrated in Fig. 1A,B was excellent and allowed for application of a ±0.7 min Rt range limit for targeted AMT quantitation. Fig. 1 also shows the high reproducibility of quantitative differences in the EIC integrals of MIPS peptide VIVLWANTER (*m*/*z* 651.3653; Fig. 1A) and IMPA1 peptide AYDFAVAVAR (*m*/*z* 541.7850; Fig. 1B) when samples from 90 ppt acclimated tilapia are compared with those from FW control fish. A heat map with EIC integrals of IMPA1 peptides shows that all diagnostic peptides are strongly increased in samples from fish exposed to 90 ppt relative to FW controls (Fig. 1C). Consolidation of the quantitative peptide data at the protein level visualizes the significantly higher abundance of MIPS (2.3-fold on average for three technical replicates) and IMPA1 (14.5-fold on average for three technical replicates) in gills from tilapia exposed to 90 ppt compared with FW handling controls (Fig. 1D).

Confirmation of MIPS and IMPA1 regulation by western blot

Upregulation of MIPS and IMPA1 was confirmed using immunoblotting with specific antibodies. Antibody specificity was verified by loading recombinant hexa-His-tagged tilapia MIPS and IMPA1. IMPA1 is readily visible on a Coomassie-stained SDS-PAGE gel just below the slightly larger hexa-His-tagged recombinant IMPA1 band (Fig. 2A). IMPA1 was much more abundant in gill epithelium from 90 ppt salinity stressed fish but was also clearly visible in the FW handling controls. In contrast, MIPS is not visible on Coomassie-stained gels, indicating that it is much less abundant in gill epithelium than IMPA1. The western blots confirm the increase in MIPS and IMPA1 that occurs after acclimation of fish to 90 ppt (Fig. 2B). They also confirm that IMPA1 increases to a much greater extent than MIPS. For MIPS, the corresponding western blot band is visible for all samples, including FW controls. This is not the case for IMPA1,

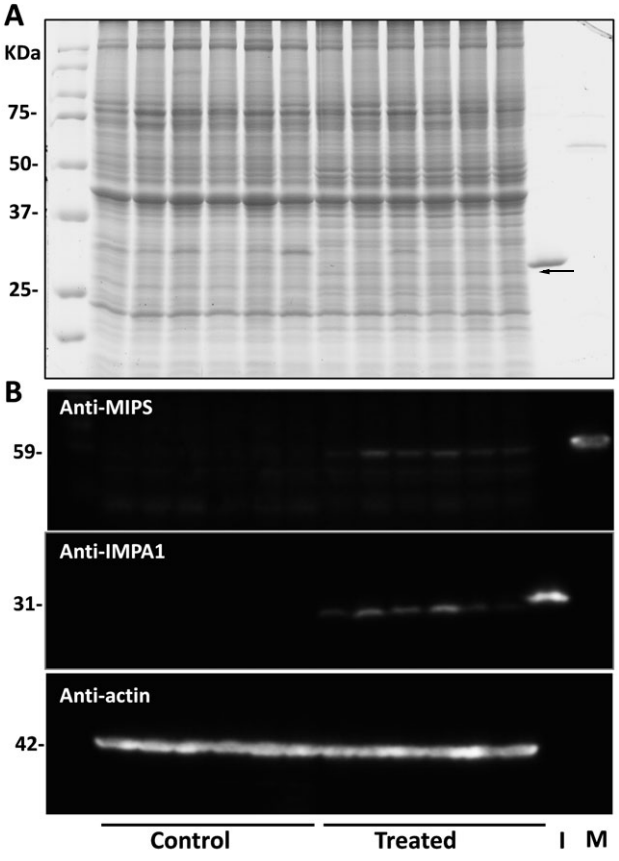

Fig. 2. MIPS and IMPA1 detection by western immunoblotting of proteins from gill epithelium of tilapia. (A) Coomassie Blue stained SDS-PAGE gel containing gill epithelial protein extract from FW handling controls and fish that were gradually acclimated from FW to 90 ppt salinity. A 15% SDS-PAGE gel was loaded with 35 µg total protein per lane. The IMPA1 band is clearly visible in the samples and is indicated by an arrow. Recombinant hexa-his-tagged *Oreochromis mossambicus* IMPA1 (I) and MIPS (M) proteins were loaded as positive controls to validate the antibodies, and molecular weight standards were also included on each gel to confirm that immunoreactive bands correspond to the expected size. (B) Western blots developed with antibodies against MIPS (top), IMPA1 (middle) and beta-actin (bottom). The actin western blot was used in addition to Coomassie staining to control for equal sample loading.

indicating that the dynamic range of western blots is more limited than that for Coomassie Blue and quantitative LC-MS/MS. The Coomassie-stained SDS-PAGE gel and the actin western blot demonstrate that equal amounts of total protein were loaded for all samples (Fig. 2).

IMPA1 and MIPS regulation during acute and moderate salinity stress

Step-wise acclimation of tilapia from FW to 90 ppt over a period of 2 weeks represents a gradual but severe salinity stress because higher salinities are not readily tolerated by this species. To assess how the MIB pathway is regulated during acute and less severe salinity stress, tilapia were acutely exposed to 34 ppt (17 ppt day^{-1}) and gradually to 70 ppt (7 ppt day^{-1}). Even though global ProfileAnalysis did not yield conclusive data for these comparisons (Table 2), targeted AMT based quantitative proteomics clearly shows that the effect of 34 ppt acute and 70 ppt gradual salinity stress on MIPS and IMPA1 is less pronounced than for 90 ppt salinity stress (Fig. 3). Nevertheless, both enzymes were significantly upregulated during 34 ppt acute salinity stress (Fig. 3A): MIPS was upregulated 2.1-fold and IMPA1 was upregulated 5.4-fold under these conditions (averages of three technical replicates). For 70 ppt gradual salinity stress, only IMPA1 was significantly upregulated (3.5-fold on average for three technical replicates) but the increase in MIPS (1.2-fold for all three technical replicates) was not statistically significant in any technical replicate (Fig. 3B). Overall, these data show that severe salinity stress, whether acute (34 ppt) or gradual (90 ppt), leads to stronger upregulation of MIB pathway enzymes than more moderate salinity stress (gradual 70 ppt).

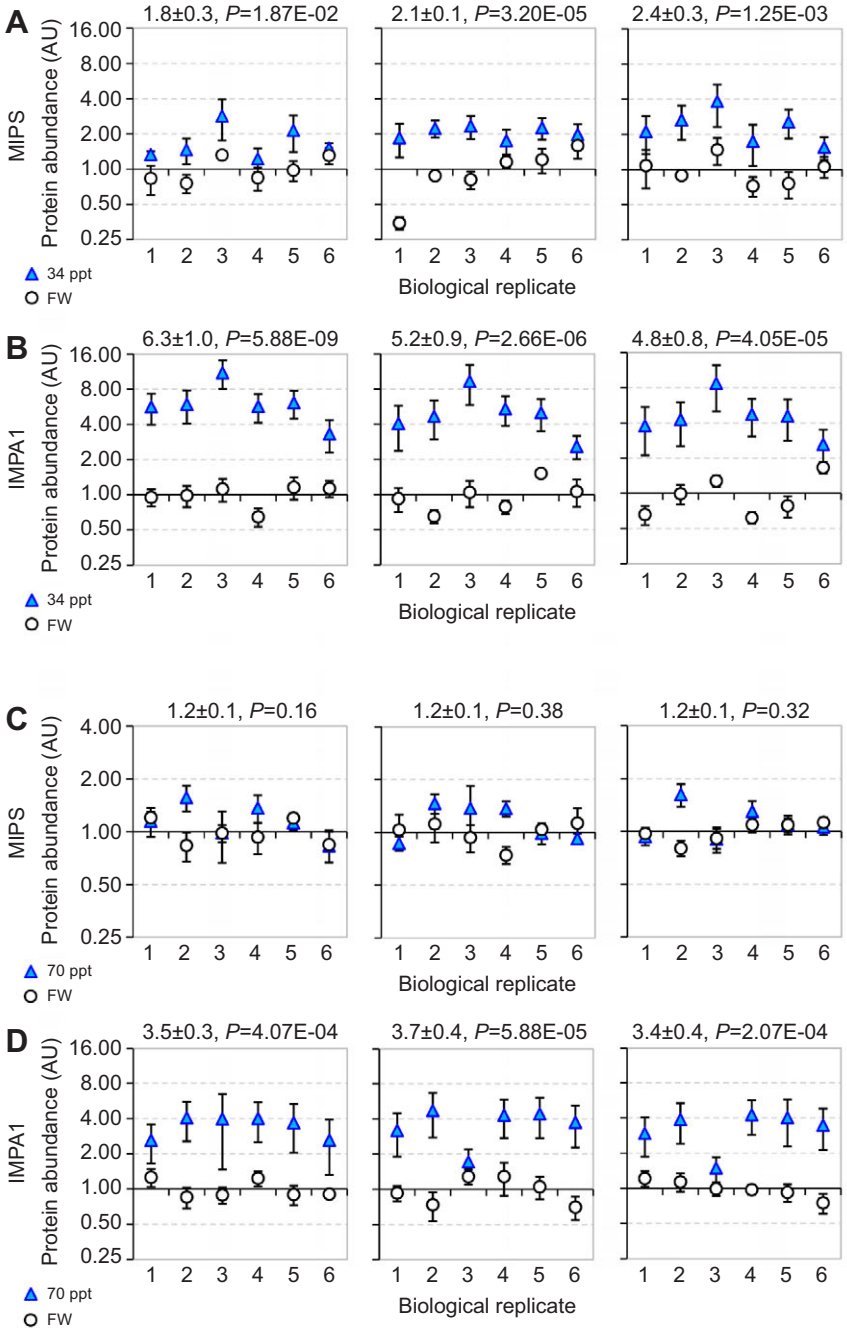

Fig. 3. Protein abundances of six biological replicates for MIPS and IMPA1 in gill epithelium of tilapia exposed to 34 ppt acute (A,B) and 70 ppt gradual (C,D) salinity stress in comparison to corresponding FW handling controls. Each data point represents the mean ± s.e.m. abundance of all diagnostic peptides for a single biological replicate, and *y*-axes are plotted on a $\log_2$ scale. Three technical replicates are depicted horizontally. The protein mean ± s.e.m. of all six biological replicates for salinity stressed fish and the *P*-value for the effect of treatment in the two-factor ANOVA are shown at the top of each chart.

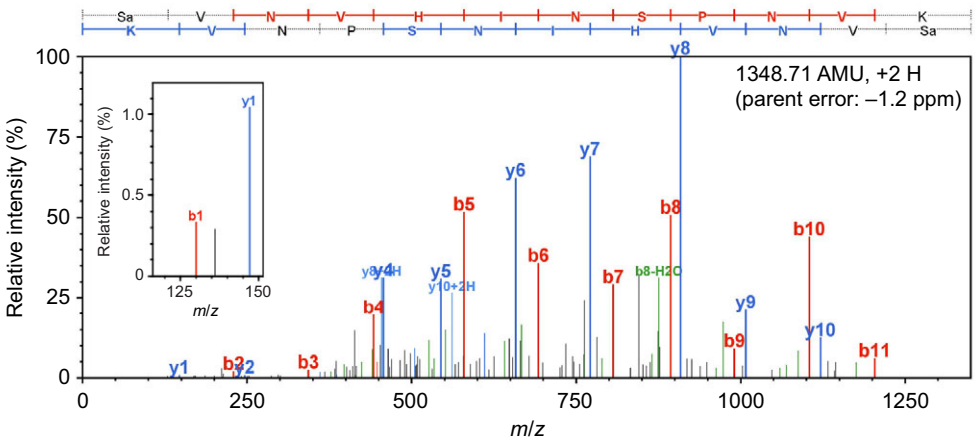

Fig. 4. Identification of the acetylated N terminus of MIPS by LC-MS/MS. A representative example of a MS/MS line spectrum of the N-terminal MIPS peptide is shown. This particular line spectrum belongs to a gill epithelium sample from tilapia acclimated to 34 ppt. Fragment ion series (b, red; y, blue) are annotated and the corresponding amino acid sequence is indicated at the top (Sa, acetyl-serine). The inset depicts a magnified portion of the MS/MS spectrum showing the presence of low-intensity b1 and y1 fragment ions.

Constitutive N-terminal acetylation of MIPS

The N-terminal peptide of MIPS was identified with high metascores by all search engines (Mascot, PEAKS, Phenyx, X!Tandem) when including protein N-terminal acetylation as a variable modification search parameter (Table 2). In contrast, neither the unmodified N-terminal MIPS peptide nor any N-terminal IMPA peptide was detected under any condition. The MS/MS spectra obtained for N-terminally acetylated MIPS peptides were of high quality and consisted of almost complete b and y ion series (Fig. 4). In addition, high A-scores (max. 250.38) were assigned to these peptides by ScaffoldPTM analysis. Furthermore, the acetyl group was localized to Ser1 with a confidence value of 100% by ScaffoldPTM. The high A-score and localization confidence values did not even consider the b1 ion, which was detectable, albeit at low intensity, and further increased the confidence of N-terminal acetylation assignment after manual inspection of the MS/MS spectra (Fig. 4). In addition, an assignment of the acetyl group to the only alternative residue in this peptide (Lys12) yielded very low scores. These data clearly demonstrate that MIPS is N-terminally acetylated. The effect of osmotic stress on N-terminal MIPS acetylation was analyzed by targeted AMT-based LC-MS/MS. The N-terminally acetylated peptide increases to a similar extent at 34 and 90 ppt (3.3- and 3.1-fold, respectively; averages of three technical replicates) as the overall protein (Fig. 5). In addition, this peptide does not change significantly at 70 ppt and is regulated in the same way as the other MIPS peptides (Fig. 5). These results, in combination with the absence of unmodified N-terminal peptide under any condition, indicate that MIPS is constitutively N-terminally acetylated. During severe salinity stress, the amount of acetylated N terminus increases in conjunction with the overall MIPS protein.

Evolutionary conservation of the MIB pathway

Because cellular *myo*-inositol accumulation in mammals is mediated *via* extracellular uptake by a sodium-*myo*-inositol cotransporter *in lieu* of MIB pathway activation (Handler and Kwon, 1993), we analyzed the degree of evolutionary sequence conservation of MIPS and IMPA in vertebrates. *Oreochromis mossambicus* MIPS cDNA is 92.4% identical to that of *O. niloticus*, 73–82% identical to that of species from other teleost orders, and 60–62% identical to mammalian MIPS (Fig. 6A). *Oreochromis mossambicus* IMPA1 is 89.3% identical to *O. niloticus* IMPA1, 66–90% identical to that of species from other teleost orders, and 61–63% identical to mammalian IMPA1 (Fig. 6B). Remarkably, whereas a single MIPS gene is present in tilapia and many other teleost genomes, MIPS is missing from the zebrafish genome (supplementary material Table S1). The *O. niloticus* genome contains four loci that encode IMPA, whereas the zebrafish genome only has a single IMPA locus (supplementary material Table S1). IMPA orthologs that correspond to *O. niloticus* IMPA1 and IMPA2 paralogs are more highly conserved across all vertebrates than the different IMPA paralogs within a single species (Fig. 6B).

Salinity regulation of MIPS, IMPA1 and IMPA2 mRNA abundance

To assess whether the salinity-induced upregulation of MIB pathway enzymes is due to regulation of the corresponding transcripts, we quantified MIPS and IMPA1 mRNA levels. In addition, we were interested in comparing how changes in protein abundance relate to changes in mRNA abundance of MIPS and IMPA1. When separating the MIPS PCR amplicons on DNA agarose gels we consistently observed two bands, one much fainter than the main band and larger in size than expected (Fig. 7A). When using genomic DNA instead of cDNA as the PCR template, only a single product that was identical to the larger cDNA amplicon was observed (Fig. 7A, Lane 10). We gel-purified and sequenced both MIPS PCR products and determined that the shorter, more abundant amplicon was missing an 86 bp (in-frame)

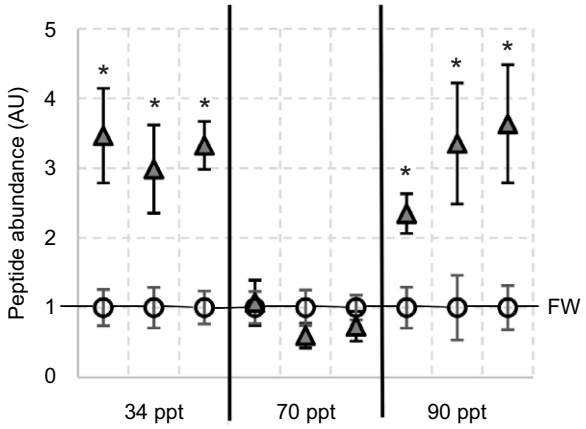

Fig. 5. Abundance of the N-terminal Ser1-acetylated MIPS peptide in gill epithelium of tilapia exposed to 34 ppt acute, 70 ppt gradual and 90 ppt gradual salinity stress (gray triangles) in comparison to the corresponding FW handling controls (open circles). Each data point represents the mean ± s.e.m. of six biological replicates, and abundances are plotted on the *y*-axis as arbitrary units (AU; $\log_2$ scale). Three technical replicates are depicted horizontally for each salinity acclimation experiment.

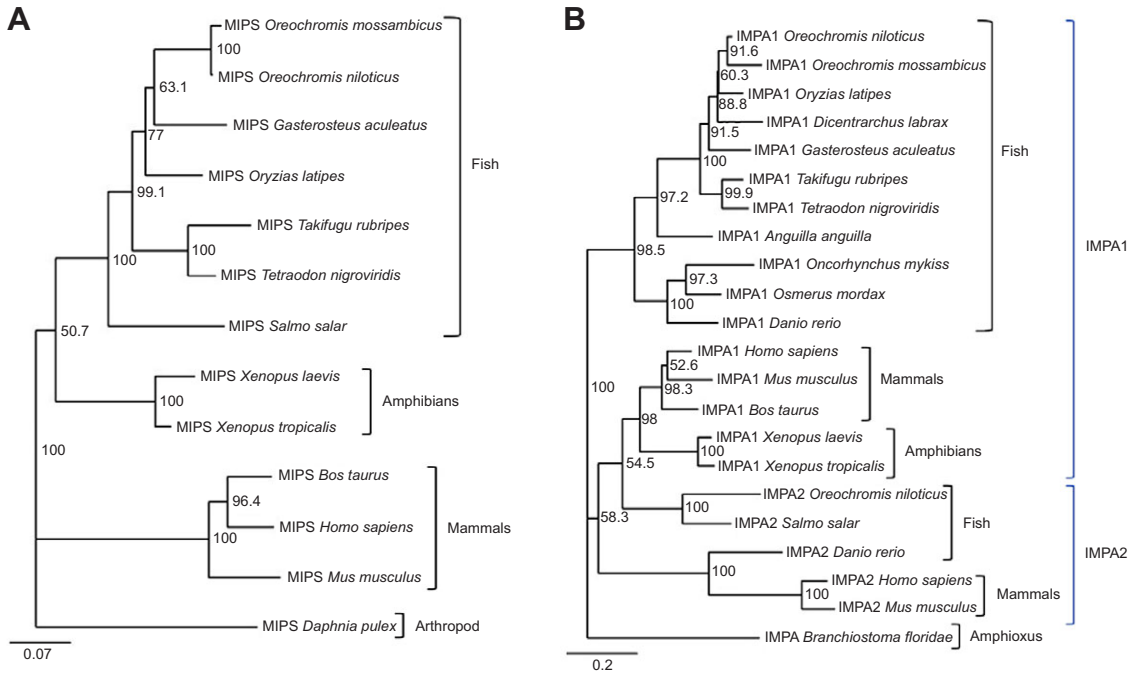

Fig. 6. Phylogenetic relationship of (A) MIPS and (B) IMPA protein sequences. Rooting of the phylogenetic trees was achieved with *Daphnia pulex* (MIPS) and *Branchiostoma floridae* (IMPA) sequences as outgroups. (A) The following NCBI/UniProt/Ensembl accession numbers were used for MIPS: *Oreochromis mossambicus* MIPS, Q1KN76; *Oreochromis niloticus* MIPS, XP_003442861; *Gasterosteus aculeatus* MIPS, ENSGACP00000013058; *Oryzias latipes* MIPS, ENSORLP00000017669; *Takifugu rubripes* MIPS, ENSTRUP00000040637; *Tetraodon nigroviridis* MIPS, ENSTNIP00000020331; *Salmo salar* MIPS, B5X3P3; *Xenopus laevis* MIPS, Q6DDT1; *Xenopus tropicalis* MIPS, F7CRT1; *Bos taurus* MIPS, Q2NL29; *Homo sapiens* MIPS, Q9NPH2; *Mus musculus* MIPS, Q9JHU9; *Daphnia pulex* MIPS, E9GTQ2. (B) The following NCBI/UniProt/Ensembl accession numbers were used for IMPA: *Oreochromis niloticus* IMPA1, XP_003439317*; Oreochromis mossambicus* IMPA1, Q3ZLD0; *Oryzias latipes* IMPA1, *Dicentrarchus labrax* IMPA1, E6ZJ93; *Gasterosteus aculeatus* IMPA1, ENSGACP00000006465; *Takifugu rubripes* IMPA1, ENSTRUP00000009117; *Tetraodon nigroviridis* IMPA1, ENSTNIP00000016661; *Anguilla anguilla* IMPA1, E1UVK7; *Oncorhynchus mykiss* IMPA1, C1BF75; *Osmerus mordax* IMPA1, C1BLV9; *Danio rerio* IMPA1, NP_001002745; *Homo sapiens* IMPA1, NP_005527; *Mus musculus* IMPA1, NP_061352; *Bos taurus* IMPA1, P20456; *Xenopus laevis* IMPA1, Q7SYT9; *Xenopus tropicalis* IMPA1, Q28FW1; *Oreochromis niloticus* IMPA2, XP_003439196; *Salmo salar* IMPA2, C0HBE4; *Danio rerio* IMPA2, NP_001018408; *Homo sapiens* IMPA2, ENSP00000269159; *Mus musculus* IMPA2, NP_444491; *Branchiostoma floridae* IMPA, XP_002597692.

fragment (Fig. 7B). Therefore, both amplicons represent MIPS transcript variants that are likely the result of alternative splicing. We designed MIPS primers that are specific for the long transcript variant to distinguish the influence of salinity acclimation on each variant (Fig. 7C). PCR products obtained with these long MIPS transcript (MIPS-250)-specific primer pairs yielded single bands on agarose gels (Fig. 7D). IMPA1 and IMPA2 amplification using specific PCR primer pairs also yielded single bands on DNA agarose gels (Table 1, gel data not shown). To allow for normalization of MIPS and IMPA mRNA levels, PCR primer pairs for beta-actin and 18S rRNA were designed, each of which produced single bands of the expected size (Table 1, gel data not shown). After optimization of qPCR conditions for MIPS, IMPA1, IMPA2, beta-actin and 18S rRNA, the corresponding C_t values had a linear relationship with sample concentration (R^2>0.996), amplification efficiency was high (85.2–98.8%) and melt curve analysis confirmed the presence of a single qPCR product in each case (supplementary material Fig. S1). Quantitative PCR showed that MIPS mRNA abundance of short and long transcript variants (MIPS-160 and MIPS-250) increased during all types of salinity stress tested (Fig. 8A). The salinity-induced increase of the major, shorter MIPS variant was much greater (28.4- to 41.1-fold) than that of the minor, longer MIPS variant (10.4- to 18.0-fold), resulting in a significant increase of the short MIPS/long MIPS ratio during salinity stress (Fig. 8B). The increase in IMPA1 mRNA abundance exceeded that of MIPS by more than an order of magnitude during all three types of salinity stress (424- to 742-fold) (Fig. 8C). In contrast, the mRNA abundance of IMPA2 increased only slightly after 34 and 90 ppt salinity acclimation and not at all after 70 ppt treatment (Fig. 5D).

DISCUSSION

Euryhaline fish tolerate large changes in salinity and the mechanisms underlying such tolerance are of interest in the context of global salinization and warming (Calvo et al., 2011; Somero, 2012). One of the few organs of euryhaline fish that is directly exposed to the external environment is the gill, and gill epithelial cells are exposed to significant osmotic stress during changes in habitat salinity. Therefore, changes in the molecular phenotype of gill epithelium in fish exposed to salinity stress provide information about the physiological mechanisms that enable euryhaline fish to cope with such stress.

Salinity effects on MIPS and IMPA1 protein abundance

Label-free quantitative proteomics was used in this study to reveal that both enzymes of the MIB pathway are regulated by salinity stress in tilapia gill epithelium. This label-free approach has several advantages over other quantitative proteomics approaches, including minimal sample manipulation, wide dynamic range, applicability to intact animals, and no ‘undersampling’ (as in spectral counting). Gill epithelium of tilapia challenged by gradual exposure to very high salinity (90 ppt) contained significantly

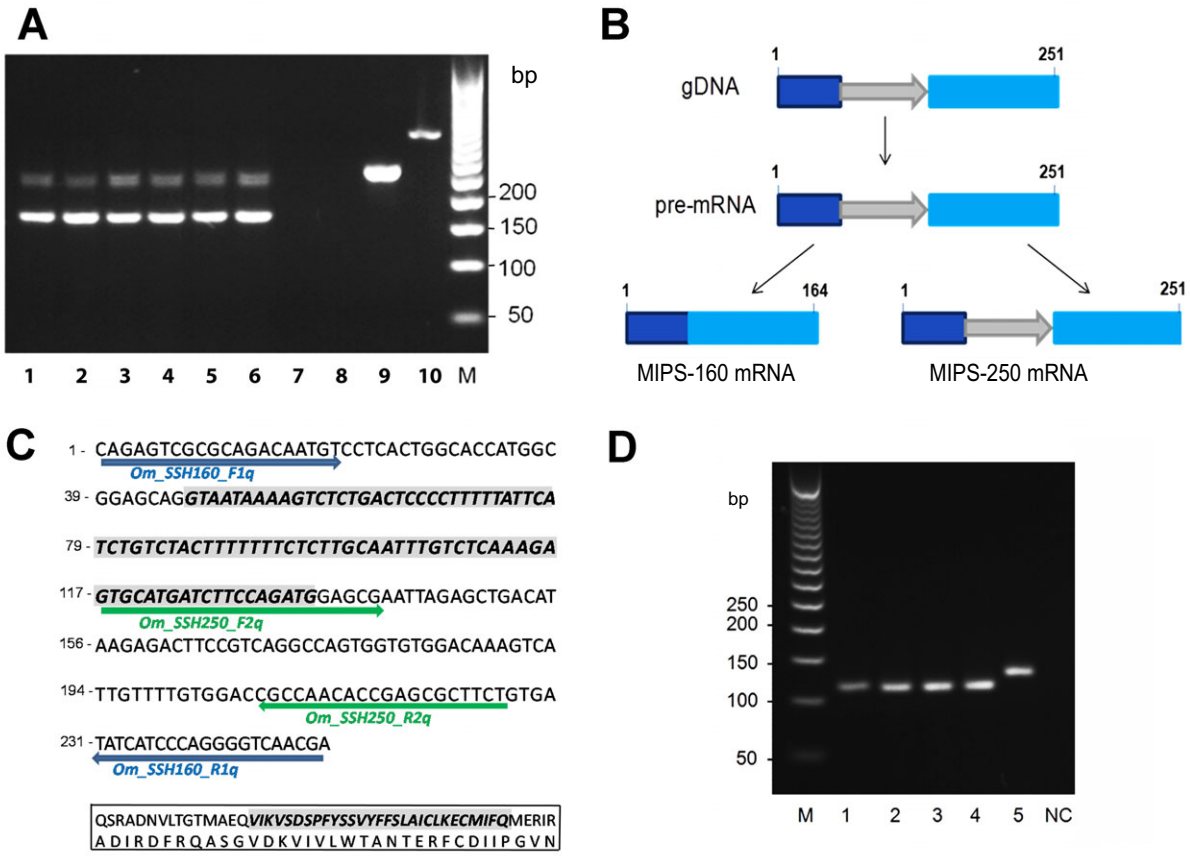

Fig. 7. Identification of alternative MIPS transcript variants in tilapia gill epithelium. (A) Amplification of MIPS cDNA using the initial set of primers yields two PCR products, but the shorter product (MIPS-160) is much more abundant than the longer product (MIPS-250). Lanes 1–5: gill RNA from different biological replicates of 70 ppt acclimated fish and treated with TURBO DNase (2U) prior to cDNA synthesis; Lane 6: control 1 indicating effectiveness of DNase treatment (gDNA was added to RNA at a 1:3 ratio, which did not affect the PCR result); Lane 7: control indicating complete removal of gDNA by DNase treatment (RNA was substituted with gDNA prior to DNase treatment and cDNA synthesis); Lane 8: negative control (no template); Lane 9: tilapia genomic DNA amplification (same as Lane 7 but without TURBO DNase treatment); Lane 10: positive RT-PCR control using HeLa cell RNA for cDNA synthesis followed by amplification of human beta-actin; Lane M: 100 bp DNA ladder. (B) Schematic representation of MIPS post-transcriptional processing due to alternative in-frame splicing of a 86 bp nucleotide fragment (indicated by a gray arrow) yielding two distinct MIPS transcripts whose PCR products are 164 and 251 bp long. (C) Sequence of the amplicons obtained using the initial MIPS primer pair and a primer that is specific for amplifying only the long transcript variant of MIPS. Annealing sites of each PCR primer are indicated as blue and green arrows, and the 86 bp fragment that distinguishes the transcript variants is shown italicized and with gray shading. The corresponding amino acid sequence is also shown italicized and with gray shading in the box below. (D) Agarose gel containing PCR products from gill cDNA samples of tilapia exposed to 34 ppt salinity stress. Lane M: 100 bp DNA ladder; Lanes 1–5: different MIPS primer pairs that are specific to only amplifying the long MIPS transcript variant (including the pair shown in C, which was selected for qPCR) yield only a single PCR product (MIPS250); Lane NC: negative PCR control (no primers).

higher levels of MIPS (EC 5.5.1.4) and IMPA1 (EC number 3.1.3.25), the two enzymes that constitute the MIB pathway (KEGG pathway number 00562, http://www.genome.jp/dbget-bin/show_pathway?map00562). However, IMPA1 protein is much more profoundly upregulated in gill epithelium of 90 ppt acclimated fish compared with FW handling controls than MIPS, which increases more moderately. Additional salinity exposure experiments (34 ppt, 70 ppt) clearly indicate that the degree of osmotic MIB pathway induction depends more on the acuteness of the salinity stress than the absolute salinity. Even though 34 ppt is only half of 70 ppt, the upregulation of MIB pathway enzymes at 34 ppt resembles that seen at 90 ppt because the salinity change was more rapid (17 ppt day^{-1} instead of 7 ppt day^{-1}) and leads to a severe osmotic stress. Gradual acclimation to 70 ppt (7 ppt day^{-1}) did not significantly increase MIPS and the increase in IMPA1 was smaller than that during the 34 and 90 ppt exposures. These data agree with the known long half-life of *myo*-inositol, which makes it suitable for accumulation as an organic osmolyte (Yancey et al., 1982). The high stability of *myo*-inositol explains why the MIB pathway is more strongly induced during acute salinity stress, when osmotic homeostasis is profoundly disturbed and the need for rapid accumulation of *myo*-inositol is greatest. Interestingly, the stability of *myo*-inositol may be affected by environmental salinity. For instance, *myo*-inositol degradation appears to be upregulated in euryhaline sharks when they are exposed to dilute seawater, which is consistent with the need to lower compatible osmolyte levels during hypo-osmotic stress (Dowd et al., 2010). Furthermore, the metabolite *myo*-inositol was shown to increase in tilapia tissues during exposure to elevated salinity, which is consistent with MIB pathway activation by salinity stress (Fiess et al., 2007).

Magnitude of MIPS *versus* IMPA1 regulation and the role of MIPS acetylation

An interesting result of this study is the large difference in the magnitude of salinity-induced upregulation of the two MIB pathway

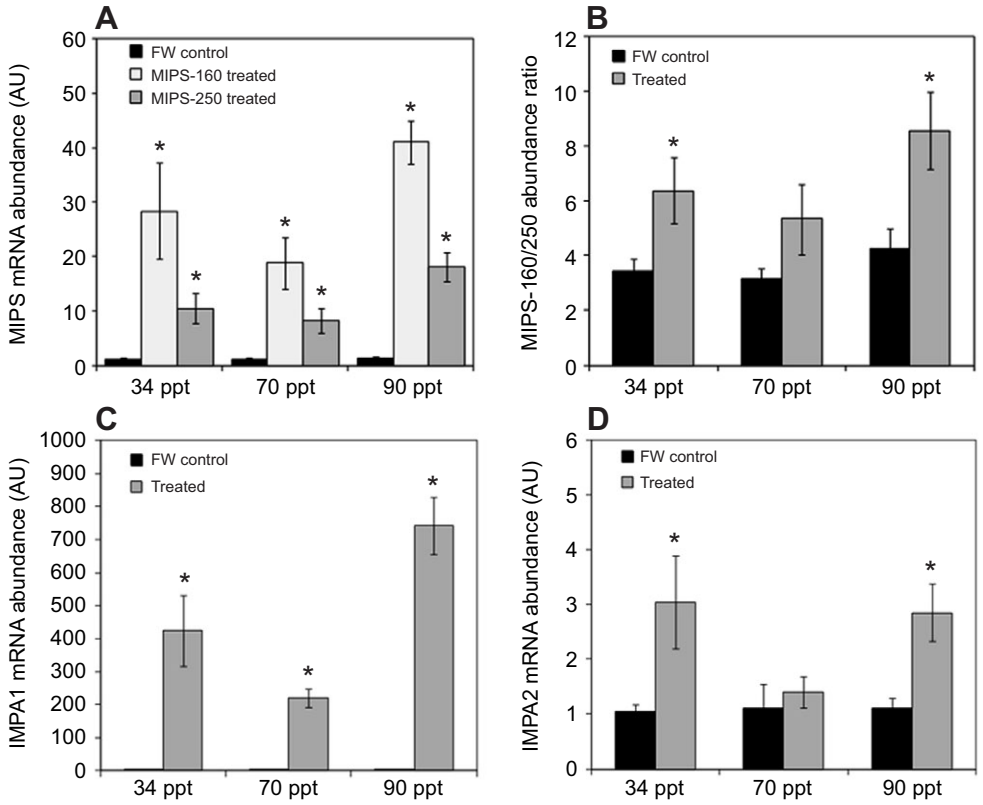

Fig. 8. Effect of salinity treatments on IMPA1 and MIPS mRNA abundance. (A) Ratio of two MIPS transcript variants for three salinity challenges relative to corresponding FW controls. (B) Salinity effects on the ratio of short *versus* long MIPS transcripts. (C) Ratio of IMPA1 transcript for three salinity challenges relative to corresponding FW controls. (D) Ratio of IMPA2 transcript for three salinity challenges relative to corresponding FW controls. All ratios were normalized against the average abundance of 18S rRNA and beta-actin mRNA. All data shown represent means ± s.e.m. (N=6). An asterisk denotes a significant difference between the salinity treatment and the corresponding control (P<0.05).

enzymes. IMPA1 is always more strongly upregulated than MIPS under our experimental conditions when environmental salinity increases, regardless of the magnitude and acuteness of salinity stress. This phenomenon can be interpreted and explained in three ways. First, during salinity stress, the catalytic efficiency of MIPS may be higher than that of IMPA1, rendering IMPA1 more rate limiting for *myo*-inositol synthesis. Second, during salinity stress, MIPS may be more stable than IMPA1 such that its turnover is slower and less *de novo* synthesis is required to replace unstable, non-functional protein that is destined for degradation. In other words, the overall MIPS protein pool in salinity-stressed gill epithelium may consist of a higher proportion of functional MIPS than is the case for IMPA1. A higher stability of MIPS may be conferred by its acetylated N terminus, which increases proportionally to the overall MIPS protein during salinity stress. The sequence and modification state of protein N termini is an important determinant of their stability and turnover rate, and this overall phenomenon has been termed the N-end rule (Bachmair et al., 1986; Varshavsky, 2011). N-terminal acetylation of proteins is known to greatly influence protein stability and degradation (Brown, 1979; Meinnel et al., 2005; Perrier et al., 2005; Clairmont et al., 2006; John et al., 2008; Gutierrez et al., 2011). Therefore, it is likely that acetylation of the MIPS N terminus serves to regulate protein stability. Because we did not detect the IMPA1 N-terminal peptide, it is possible that this peptide harbors multiple modifications such as ubiquitination and others that render IMPA1 less stable and are difficult to detect using conventional search strategies. Allowing too many variable modifications during MS/MS peptide and protein identification searches greatly increases the search space and false discovery rate and is, therefore, impractical. A third possible reason for the observed difference in the magnitude of salinity-induction of MIPS *versus* IMPA1 is the capacity of IMPA1 to utilize alternative substrates. In addition to utilizing *myo*-inositol-3-phosphate produced by MIPS, IMPA1 can also convert *myo*-inositol-1-phosphate and *myo*-inositol-4-phosphate (produced by enzymes other than MIPS) to *myo*-inositol (Gee et al., 1988; Seelan et al., 2009; Sato et al., 2011) (see KEGG map 00562).

MIPS/IMPA mRNA *versus* protein regulation

The overall effects of different salinity challenges on MIPS and IMPA1 abundance are qualitatively similar at the mRNA and protein levels. The greatest effect is evident at 90 ppt, the lowest at 70 ppt, and salinity stress has a much more pronounced effect on IMPA1 than MIPS at both mRNA and protein levels. However, both MIPS mRNA variants significantly increase even during 70 ppt acclimation, which is not reflected at the protein level. This difference between mRNA and protein levels may be attributed to an inhibitory effect of salinity stress on protein synthesis and translational efficiency (Kültz, 1996; Burkewitz et al., 2012). Inhibition of protein synthesis/translational efficiency during salinity stress would also explain the much higher levels of mRNA induction at 34 and 90 ppt compared with the magnitude of the corresponding protein increase. Stronger increases in mRNA compared with corresponding protein abundances in response to stress are not uncommon and have been observed for many other systems (Kaufmann and van Oudenaarden, 2007; Persson et al., 2009; Shebl et al., 2010; Schwanhäusser et al., 2011).

Interestingly, two different MIPS mRNA variants are present in tilapia gill epithelium. Both variants are induced by salinity stress but the shorter variant is upregulated approximately twice as much as the longer MIPS variant. These data indicate a potential role of alternative MIPS splicing during salinity stress. Alternative splicing of another strongly salinity-regulated protein (Na-K-2Cl cotransporter) has been implicated in sensing and responding to different severities of osmotic stress in mammals (Castrop and Schnermann, 2008). In contrast to MIPS, two IMPA isoforms that

are encoded by distinct genes are expressed in gill epithelium. IMPA1 is highly expressed and strongly regulated by salinity, whereas IMPA2 mRNA levels are much lower and only moderately increase at 34 and 90 ppt. Evidence for salinity-dependent regulation of IMPA1 mRNA has recently been reported for other species of euryhaline fish, suggesting that the induction of the MIB pathway during hyperosmotic stress is an evolutionarily conserved trait of euryhaline teleosts. In European eel (*Anguilla anguilla*), IMPA1 mRNA increases in parallel to increased salinity (Kalujnaia and Cramb, 2009; Kalujnaia et al., 2010), and in killifish (*Fundulus heteroclitus*), IMPA1 mRNA is downregulated in response to a salinity decrease (Whitehead et al., 2012). The exquisite osmotic sensitivity of IMPA1 at both mRNA and protein levels makes this enzyme a robust indicator system for mechanistic studies of osmosensory signal transduction.

Evolutionary implications of the MIB pathway for salinity tolerance of fish

Our finding that IMPA orthologs representing IMPA1 or IMPA2 paralogs are more highly conserved across all vertebrates than the different IMPA paralogs within a single species suggests that a gene duplication event giving rise to IMPA1 and IMPA2 paralogs has occurred early during vertebrate evolution. Additional gene duplication events producing more than two IMPA paralogs may have only occurred in particular vertebrate lineages. Alternatively, extra IMPA copies may have been lost in many vertebrate lineages because of a lack of selection pressure for retaining them. From an evolutionary perspective it is also very interesting to note that stenohaline zebrafish, which do not tolerate significant salinity stress (>10 ppt), lack a MIPS gene, suggesting that they are unable to synthesize the compatible osmolyte *myo*-inositol from glucose-6-phosphate *via* the MIB pathway. Moreover, our study shows that euryhaline tilapia have four different IMPA genes, compared with only a single IMPA gene encoded in the zebrafish genome. We interpret these data as evidence for a significant role of the MIB pathway during evolution of the physiological trait of euryhalinity in fishes. Surprisingly, in mammals, the MIB pathway does not seem to play a significant role for accumulation of *myo*-inositol during hyperosmotic stress even though most mammalian genomes contain the necessary enzymes. Instead, mammalian cells accumulate *myo*-inositol *via* uptake by a sodium-coupled co-transporter (Handler and Kwon, 1993). The reason for this shift from synthesis to uptake of *myo*-inositol is unknown, but may include tissue-specific constraints (gills are specific to fishes but absent in mammals).

In summary, we have shown that the MIB pathway is strongly regulated by environmental salinity in euryhaline tilapia. Hyperosmotic upregulation of both MIB pathway enzymes (MIPS and IMPA) is proportional to the severity of salinity stress and is evident at both mRNA and protein levels. The magnitude of upregulation is much higher at the mRNA than the protein level, which we interpret as evidence for an inhibitory effect of salinity stress on protein synthesis/translational efficiency. Tilapia have a single MIPS gene, which is expressed in gill epithelium as two splice variants that are present in different amounts and differ in their responsiveness to salinity stress. Tilapia have four IMPA genes, but only two are expressed in gill epithelium and only IMPA1 is highly expressed and very strongly regulated by salinity. The effect of salinity stress is less pronounced on MIPS than on IMPA1, which may be (at least partly) due to constitutive N-terminal acetylation. Based on these data and the absence of a functional MIB pathway in zebrafish, we conclude that this pathway represents a critical prerequisite for the evolution of euryhalinity in fish.

ACKNOWLEDGEMENTS

We are grateful to James Krause, Katherine Ridenour and Emily Chan for their help with fish maintenance and acclimation. We also thank the Bruker Daltonics (Bremen, Germany) technical support team, in particular Wolfgang Jabs, Henri O'Connor and Peter Hufnagel, for invaluable technical assistance.

AUTHOR CONTRIBUTIONS

R.S. performed animal acclimation, cloning, mRNA and western blot experiments, analyzed and interpreted the data, and wrote large parts of the manuscript. D.K. designed the study, performed the proteomics experiments, analyzed and interpreted the data, and contributed to manuscript writing and editing. F.V. expressed and purified recombinant MIPS and IMPA1. J.L. extracted gill protein and prepared samples for proteomics. A.M.G., F.V. and J.L. all participated in animal acclimation experiments, sample preparation, data analysis, and manuscript editing.

COMPETING INTERESTS

No competing interests declared.

FUNDING

This work was supported by the National Science Foundation [grant number IOS-1049780 to D.K.] and the National Institute of Environmental Health Sciences [grant number P42ES004699, project B to D.K.]. Deposited in PMC for release after 12 months.

REFERENCES

Andreev, V. P., Petyuk, V. A., Brewer, H. M., Karpievitch, Y. V., Xie, F., Clarke, J., Camp, D., Smith, R. D., Lieberman, A. P., Albin, R. L. et al. (2012). Label-free quantitative LC-MS proteomics of Alzheimer's disease and normally aged human brains. *J. Proteome Res.* **11**, 3053-3067.

Bachmair, A., Finley, D. and Varshavsky, A. (1986). *In vivo* half-life of a protein is a function of its amino-terminal residue. *Science* **234**, 179-186.

Beausoleil, S. A., Villén, J., Gerber, S. A., Rush, J. and Gygi, S. P. (2006). A probability-based approach for high-throughput protein phosphorylation analysis and site localization. *Nat. Biotechnol.* **24**, 1285-1292.

Binz, P. A., Barkovich, R., Beavis, R. C., Creasy, D., Horn, D. M., Julian, R. K., Jr, Seymour, S. L., Taylor, C. F. and Vandenbrouck, Y. (2008). Guidelines for reporting the use of mass spectrometry informatics in proteomics. *Nat. Biotechnol.* **26**, 862.

Brown, J. L. (1979). A comparison of the turnover of alpha-N-acetylated and nonacetylated mouse L-cell proteins. *J. Biol. Chem.* **254**, 1447-1449.

Burkewitz, K., Choe, K. P., Lee, E. C., Deonarine, A. and Strange, K. (2012). Characterization of the proteostasis roles of glycerol accumulation, protein degradation and protein synthesis during osmotic stress in *C. elegans*. *PLoS ONE* **7**, e34153.

Calvo, E., Simo, R., Coma, R., Ribes, M., Pascual, J., Sabates, A., Gili, J. M. and Pelejero, C. (2011). Effects of climate change on Mediterranean marine ecosystems: the case of the Catalan Sea. *Clim. Res.* **50**, 1-29.

Castrop, H. and Schnermann, J. (2008). Isoforms of renal Na-K-2Cl cotransporter NKCC2: expression and functional significance. *Am. J. Physiol.* **295**, F859-F866.

Clairmont, K. B., Buckholz, T. M., Pellegrino, C. M., Buxton, J. M., Barucci, N., Bell, A., Ha, S., Li, F., Claus, T. H., Salhanick, A. I. et al. (2006). Engineering of a VPAC2 receptor peptide agonist to impart dipeptidyl peptidase IV stability and enhance *in vivo* glucose disposal. *J. Med. Chem.* **49**, 7545-7548.

Costa-Pierce, B. A. (2003). Rapid evolution of an established feral tilapia (*Oreochromis* spp.): the need to incorporate invasion science into regulatory structures. *Biol. Invasions* **5**, 71-84.

Côté, R. G., Griss, J., Dianes, J. A., Wang, R., Wright, J. C., van den Toorn, H. W., van Breukelen, B., Heck, A. J., Hulstaert, N., Martens, L. et al. (2012). The PRoteomics IDEntification (PRIDE) Converter 2 framework: an improved suite of tools to facilitate data submission to the PRIDE database and the ProteomeXchange consortium. *Mol. Cell. Proteomics* **11**, 1682-1689.

Craig, R. and Beavis, R. C. (2004). TANDEM: matching proteins with tandem mass spectra. *Bioinformatics* **20**, 1466-1467.

Csordas, A., Ovelleiro, D., Wang, R., Foster, J. M., Ríos, D., Vizcaíno, J. A. and Hermjakob, H. (2012). PRIDE: quality control in a proteomics data repository. *Database* **2012**, bas004.

Csordas, A., Wang, R., Ríos, D., Reisinger, F., Foster, J. M., Slotta, D. J., Vizcaíno, J. A. and Hermjakob, H. (2013). From Peptidome to PRIDE: public proteomics data migration at a large scale. *Proteomics* **13**, 1692-1695.

Cutillas, P. R. and Vanhaesebroeck, B. (2007). Quantitative profile of five murine core proteomes using label-free functional proteomics. *Mol. Cell. Proteomics* **6**, 1560-1573.

Dowd, W. W., Harris, B. N., Cech, J. J., Jr and Kültz, D. (2010). Proteomic and physiological responses of leopard sharks (*Triakis semifasciata*) to salinity change. *J. Exp. Biol.* **213**, 210-224.

Evans, T. G. and Somero, G. N. (2008). A microarray-based transcriptomic time-course of hyper- and hypo-osmotic stress signaling events in the euryhaline fish *Gillichthys mirabilis*: osmosensors to effectors. *J. Exp. Biol.* **211**, 3636-3649.

Fiess, J. C., Kunkel-Patterson, A., Mathias, L., Riley, L. G., Yancey, P. H., Hirano, T. and Grau, E. G. (2007). Effects of environmental salinity and temperature on osmoregulatory ability, organic osmolytes, and plasma hormone profiles in the Mozambique tilapia (*Oreochromis mossambicus*). *Comp. Biochem. Physiol.* **146A**, 252-264.

Fiol, D. F., Chan, S. Y. and Kültz, D. (2006). Identification and pathway analysis of immediate hyperosmotic stress responsive molecular mechanisms in tilapia (*Oreochromis mossambicus*) gill. *Comp. Biochem. Physiol.* **1D**, 344-356.

Fiol, D. F., Mak, S. K. and Kültz, D. (2007). Specific TSC22 domain transcripts are hypertonically induced and alternatively spliced to protect mouse kidney cells during osmotic stress. *FEBS J.* **274**, 109-124.
Fiol, D. F., Sanmarti, E., Sacchi, R. and Kültz, D. (2009). A novel tilapia prolactin receptor is functionally distinct from its paralog. *J. Exp. Biol.* **212**, 2007-2015.
Flick, K. and Kaiser, P. (2012). Protein degradation and the stress response. *Semin. Cell Dev. Biol.* **23**, 515-522.
Gee, N. S., Ragan, C. I., Watling, K. J., Aspley, S., Jackson, R. G., Reid, G. G., Gani, D. and Shute, J. K. (1988). The purification and properties of myo-inositol monophosphatase from bovine brain. *Biochem. J.* **249**, 883-889.
Gracey, A. Y., Troll, J. V. and Somero, G. N. (2001). Hypoxia-induced gene expression profiling in the euryoxic fish *Gillichthys mirabilis*. *Proc. Natl. Acad. Sci. USA* **98**, 1993-1998.
Gutierrez, D. B., Garland, D. and Schey, K. L. (2011). Spatial analysis of human lens aquaporin-0 post-translational modifications by MALDI mass spectrometry tissue profiling. *Exp. Eye Res.* **93**, 912-920.
Handler, J. S. and Kwon, H. M. (1993). Regulation of renal cell organic osmolyte transport by tonicity. *Am. J. Physiol.* **265**, C1449-C1455.
John, H., Maronde, E., Forssmann, W. G., Meyer, M. and Adermann, K. (2008). N-terminal acetylation protects glucagon-like peptide GLP-1-(7-34)-amide from DPP-IV-mediated degradation retaining cAMP- and insulin-releasing capacity. *Eur. J. Med. Res.* **13**, 73-78.
Kalujnaia, S. and Cramb, G. (2009). Regulation of expression of the myo-inositol monophosphatase 1 gene in osmoregulatory tissues of the European eel *Anguilla anguilla* after seawater acclimation. *Ann. New York Acad. Sci.* **1163**, 433-436.
Kalujnaia, S., McVee, J., Kasciukovic, T., Stewart, A. J. and Cramb, G. (2010). A role for inositol monophosphatase 1 (IMPA1) in salinity adaptation in the euryhaline eel (*Anguilla anguilla*). *FASEB J.* **24**, 3981-3991.
Kaufmann, B. B. and van Oudenaarden, A. (2007). Stochastic gene expression: from single molecules to the proteome. *Curr. Opin. Genet. Dev.* **17**, 107-112.
Koenig, T., Menze, B. H., Kirchner, M., Monigatti, F., Parker, K. C., Patterson, T., Steen, J. J., Hamprecht, F. A. and Steen, H. (2008). Robust prediction of the MASCOT score for an improved quality assessment in mass spectrometric proteomics. *J. Proteome Res.* **7**, 3708-3717.
Kültz, D. (1996). Plasticity and stressor specificity of osmotic and heat shock responses of *Gillichthys mirabilis* gill cells. *Am. J. Physiol.* **271**, C1181-C1193.
Kültz, D. and Avila, K. (2001). Mitogen-activated protein kinases are *in vivo* transducers of osmosensory signals in fish gill cells. *Comp. Biochem. Physiol.* **129B**, 821-829.
Kültz, D. and Burg, M. (1998). Evolution of osmotic stress signaling *via* MAP kinase cascades. *J. Exp. Biol.* **201**, 3015-3021.
Kültz, D., Li, J., Gardell, A. M. and Sacchi, R. (2013). Quantitative molecular phenotyping of tilapia (*Oreochromis mossambicus*) gill remodeling in response to salinity stress. *Mol. Cell. Proteomics* [Epub ahead of print] doi:10.1074/mcp.M113.029827.
Marshall, W. S., Watters, K. D., Hovdestad, L. R., Cozzi, R. R. and Katoh, F. (2009). CFTR Cl^- channel functional regulation by phosphorylation of focal adhesion kinase at tyrosine 407 in osmosensitive ion transporting mitochondria rich cells of euryhaline killifish. *J. Exp. Biol.* **212**, 2365-2377.
Masselot, A., Binz, P.-A., Cambria, L. and Appel, R. D. (2004). Phenyx: combining high-throughput and pertinence in protein identification. *Mol. Cell. Proteomics* **3**, S257.
Matzke, M. M., Brown, J. N., Gritsenko, M. A., Metz, T. O., Pounds, J. G., Rodland, K. D., Shukla, A. K., Smith, R. D., Waters, K. M., McDermott, J. E. et al. (2013). A comparative analysis of computational approaches to relative protein quantification using peptide peak intensities in label-free LC-MS proteomics experiments. *Proteomics* **13**, 493-503.
Meinnel, T., Peynot, P. and Giglione, C. (2005). Processed N-termini of mature proteins in higher eukaryotes and their major contribution to dynamic proteomics. *Biochimie* **87**, 701-712.
Miles, K. A., Ricca, M. A., Meckstroth, A. and Spring, S. E. (2009). *Salton Sea Ecosystem Monitoring Project: Open-File Report 1276*, pp. 1-150. US Department of the Interior, USGS.
Munnik, T. and Vermeer, J. E. (2010). Osmotic stress-induced phosphoinositide and inositol phosphate signalling in plants. *Plant Cell Environ.* **33**, 655-669.
Perrier, J., Durand, A., Giardina, T. and Puigserver, A. (2005). Catabolism of intracellular N-terminal acetylated proteins: involvement of acylpeptide hydrolase and acylase. *Biochimie* **87**, 673-685.
Persson, O., Brynnel, U., Levander, F., Widegren, B., Salford, L. G. and Krogh, M. (2009). Proteomic expression analysis and comparison of protein and mRNA expression profiles in human malignant gliomas. *Proteomics Clin. Appl.* **3**, 83-94.
Pfaffl, M. W. (2001). A new mathematical model for relative quantification in real-time RT-PCR. *Nucleic Acids Res.* **29**, e45.
Ruijter, J. M., Ramakers, C., Hoogaars, W. M., Karlen, Y., Bakker, O., van den Hoff, M. J. and Moorman, A. F. (2009). Amplification efficiency: linking baseline and bias in the analysis of quantitative PCR data. *Nucleic Acids Res.* **37**, e45.
Sardella, B. A. and Brauner, C. J. (2007). Cold temperature-induced osmoregulatory failure: the physiological basis for tilapia winter mortality in the Salton Sea? *Calif. Fish Game* **93**, 200-213.
Sardella, B. A., Matey, V., Cooper, J., Gonzalez, R. J. and Brauner, C. J. (2004). Physiological, biochemical and morphological indicators of osmoregulatory stress in 'California' Mozambique tilapia (*Oreochromis mossambicus* × *O. urolepis hornorum*) exposed to hypersaline water. *J. Exp. Biol.* **207**, 1399-1413.
Sato, Y., Yazawa, K., Yoshida, S., Tamaoki, M., Nakajima, N., Iwai, H., Ishii, T. and Satoh, S. (2011). Expression and functions of *myo*-inositol monophosphatase family genes in seed development of Arabidopsis. *J. Plant Res.* **124**, 385-394.
Schwanhäusser, B., Busse, D., Li, N., Dittmar, G., Schuchhardt, J., Wolf, J., Chen, W. and Selbach, M. (2011). Global quantification of mammalian gene expression control. *Nature* **473**, 337-342.
Schwanhäusser, B., Wolf, J., Selbach, M. and Busse, D. (2013). Synthesis and degradation jointly determine the responsiveness of the cellular proteome. *Bioessays* **35**, 597-601.
Searle, B. C. and Turner, M. (2006). Improving computer interpretation of linear ion trap proteomics data using Scaffold. *Mol. Cell. Proteomics* **5**, S297.
Seelan, R. S., Lakshmanan, J., Casanova, M. F. and Parthasarathy, R. N. (2009). Identification of myo-inositol-3-phosphate synthase isoforms: characterization, expression, and putative role of a 16-kDa γ_c isoform. *J. Biol. Chem.* **284**, 9443-9457.
Selbach, M., Schwanhäusser, B., Thierfelder, N., Fang, Z., Khanin, R. and Rajewsky, N. (2008). Widespread changes in protein synthesis induced by microRNAs. *Nature* **455**, 58-63.
Shebl, F. M., Pinto, L. A., García-Piñeres, A., Lempicki, R., Williams, M., Harro, C. and Hildesheim, A. (2010). Comparison of mRNA and protein measures of cytokines following vaccination with human papillomavirus-16 L1 virus-like particles. *Cancer Epidemiol. Biomarkers Prev.* **19**, 978-981.
Somero, G. N. (2012). The physiology of global change: linking patterns to mechanisms. *Ann. Rev. Mar. Sci.* **4**, 39-61.
Stickney, R. R. (1986). Tilapia tolerance of saline waters: a review. *Prog. Fish-Cult.* **48**, 161-167.
Taylor, C. F., Paton, N. W., Lilley, K. S., Binz, P. A., Julian, R. K., Jr, Jones, A. R., Zhu, W., Apweiler, R., Aebersold, R., Deutsch, E. W. et al. (2007). The minimum information about a proteomics experiment (MIAPE). *Nat. Biotechnol.* **25**, 887-893.
Taylor, C. F., Binz, P. A., Aebersold, R., Affolter, M., Barkovich, R., Deutsch, E. W., Horn, D. M., Hühmer, A., Kussmann, M., Lilley, K. et al. (2008). Guidelines for reporting the use of mass spectrometry in proteomics. *Nat. Biotechnol.* **26**, 860-861.
Varshavsky, A. (2011). The N-end rule pathway and regulation by proteolysis. *Protein Sci.* **20**, 1298-1345.
Vizcaíno, J. A., Côté, R. G., Csordas, A., Dianes, J. A., Fabregat, A., Foster, J. M., Griss, J., Alpi, E., Birim, M., Contell, J. et al. (2013). The PRoteomics IDEntifications (PRIDE) database and associated tools: status in 2013. *Nucleic Acids Res.* **41**, D1063-D1069.
Wang, R., Fabregat, A., Ríos, D., Ovelleiro, D., Foster, J. M., Côté, R. G., Griss, J., Csordas, A., Perez-Riverol, Y., Reisinger, F. et al. (2012). PRIDE Inspector: a tool to visualize and validate MS proteomics data. *Nat. Biotechnol.* **30**, 135-137.
Whitehead, A., Roach, J. L., Zhang, S. and Galvez, F. (2012). Salinity- and population-dependent genome regulatory response during osmotic acclimation in the killifish (*Fundulus heteroclitus*) gill. *J. Exp. Biol.* **215**, 1293-1305.
Yancey, P. H., Clark, M. E., Hand, S. C., Bowlus, R. D. and Somero, G. N. (1982). Living with water stress: evolution of osmolyte systems. *Science* **217**, 1214-1222.
Zhang, J., Xin, L., Shan, B. Z., Chen, W. W., Xie, M. J., Yuen, D., Zhang, W. M., Zhang, Z. F., Lajoie, G. A. and Ma, B. (2012). PEAKS DB: *de novo* sequencing assisted database search for sensitive and accurate peptide identification. *Mol. Cell. Proteomics* **11**, M111.010587.

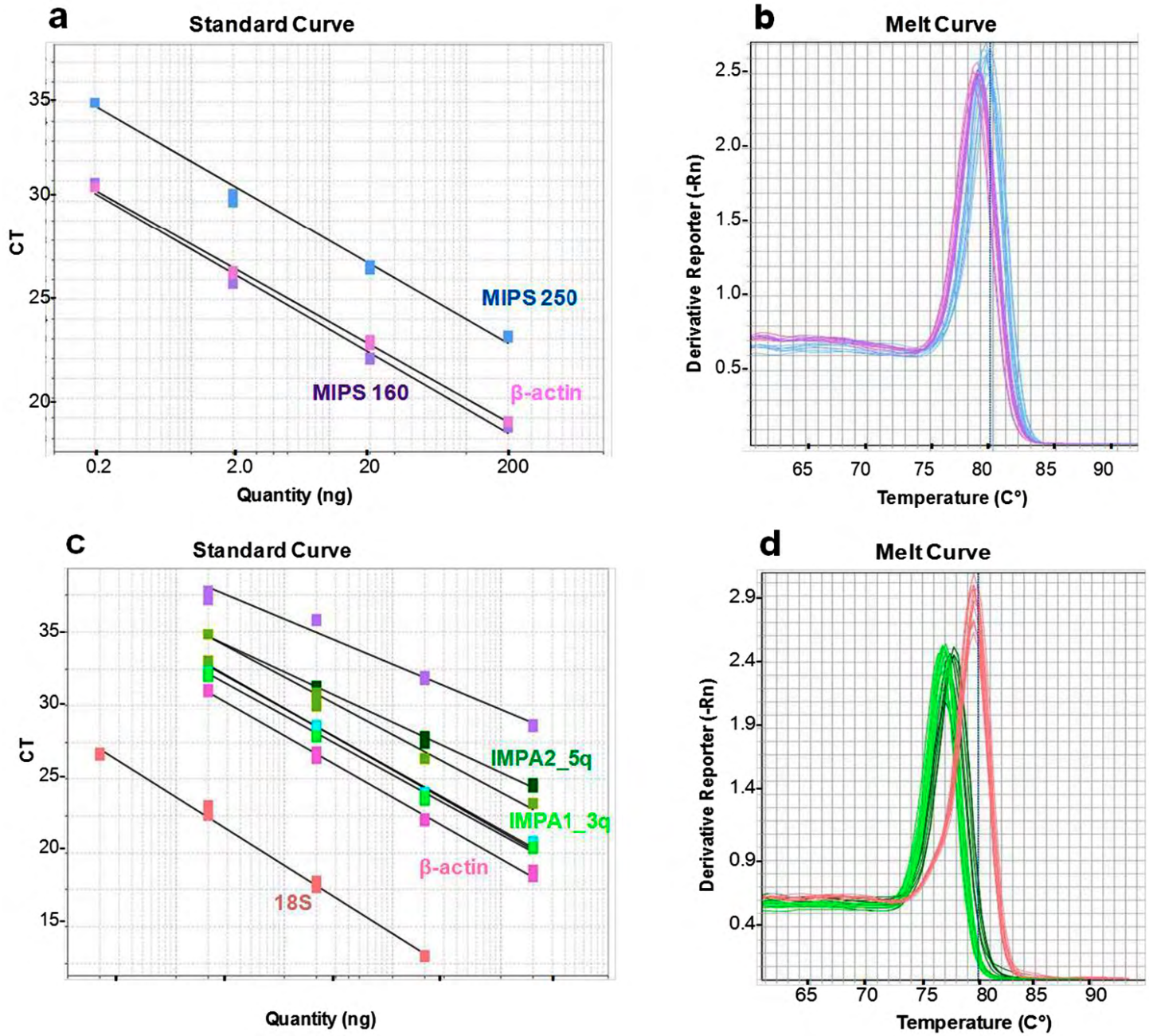

Fig. S1. Optimization of quantitative PCR (qPCR) conditions for MIPS, IMPA1, IMPA2, beta-actin and 18S cDNA quantitation. PCR amplification efficiencies were calculated from the slopes of standard curves and were higher than 90% with R^2>0.997. Melt curve analysis showed a single peak for all primers and dilutions tested indicating that each reaction resulted in a single predominant PCR product. (A) Standard curve using different starting concentrations (*x*-axis) and primer pairs for long and short MIPS transcripts and beta-actin. (B) Melt curve analysis of MIPS and beta-actin qPCR products. (C) Standard curve using different starting concentrations (*x*-axis) and primer pairs for IMPA1, IMPA2 and 18S cDNAs. IMPA primer pairs selected for qPCR analyses of all samples are labeled in green. (D) Melt curve analysis of IMPA1, IMPA2 and 18S qPCR products.

Table S1. Results of sequence similarity searches using discontigous megablast and *Oreochromis mossambicus* MIPS (Genbank AC DQ465381) and IMPA1 (Genbank AC JQ943581) cDNA sequences as templates against the RefSeq genomes (blue) and transcriptomes (black) of *Oreochromis niloticus* and *Danio rerio* (Genbank, 06 July 2013)

Query Sequence	Matched Locus	Max. Score	Total Score	Query Coverage
gi|93115135|gb|DQ465381.1|	Oreochromis niloticus unplaced genomic scaffold, Orenil1.0 scaffold00021, whole genome shotgun sequence	883	3664	99%
gi|93115135|gb|DQ465381.1|	PREDICTED: Oreochromis niloticus inositol-3-phosphate synthase 1-B-like (LOC100704062), mRNA	1450	2775	75%
gi|425895518|gb|JQ943581.1|	Oreochromis niloticus unplaced genomic scaffold, Orenil1.0 scaffold00006, whole genome shotgun sequence	318	1864	96%
gi|425895518|gb|JQ943581.1|	Oreochromis niloticus unplaced genomic scaffold, Orenil1.0 scaffold00284, whole genome shotgun sequence	77	288	33%
gi|425895518|gb|JQ943581.1|	PREDICTED: Oreochromis niloticus inositol monophosphatase 1-like (LOC100696589), mRNA	1496	1496	88%
gi|425895518|gb|JQ943581.1|	PREDICTED: Oreochromis niloticus inositol monophosphatase 1-like (LOC100708678), mRNA	192	192	58%
gi|425895518|gb|JQ943581.1|	PREDICTED: Oreochromis niloticus inositol monophosphatase 1-like (LOC100712427), mRNA	188	188	49%
gi|425895518|gb|JQ943581.1|	PREDICTED: Oreochromis niloticus inositol monophosphatase 1-like (LOC100689806), mRNA	89.7	89.7	23%
gi|425895518|gb|JQ943581.1|	Danio rerio strain Tuebingen chromosome 2 genomic scaffold, Zv9_scaffold202	107	259	34%
gi|425895518|gb|JQ943581.1|	Danio rerio inositol(myo)-1(or 4)-monophosphatase 1 (impa1), mRNA >gb|BC076438.1| Danio rerio inositol(myo)-1(or 4)-monophosphatase 1, mRNA (cDNA clone MGC:100926 IMAGE:7145589), complete cds	347	347	0.78